THE JOURNAL OF PHYSICAL CHEMISTRY B

Article

pubs.acs.org/JPCB

Investigation of Ethanol–Peptide and Water–Peptide Interactions through Intermolecular Nuclear Overhauser Effects and Molecular Dynamics Simulations

J. T. Gerig*

Department of Chemistry & Biochemistry, University of California, Santa Barbara, Santa Barbara, California 93106, United States

Supporting Information

ABSTRACT: Molecular dynamics simulations have been used to explore solvent–solute intermolecular nuclear Overhauser effects (NOEs) on NMR (nuclear magnetic resonance) signals of [val5]angiotensin dissolved in 35% ethanol–water (v/v). Consideration of chemical shift, coupling constant and intramolecular NOE data suggest that conformations of the peptide are adequately sampled by simulations of up to 0.6 μs duration. Calculated cross relaxation terms at 0 and 25 °C are compared to experimental values and to terms predicted using a particulate model of the solvent. Many calculated solvent NOEs are in agreement with experimental results; disagreements are particularly striking for hydrogens of the Phe8 residue of the peptide. Calculations show that individual molecules of either solvent component can spend many ns in association with the peptide but dipolar interactions within such a complex account for only a few percent of an observed cross relaxation rate. Most parts of the peptide interact selectively with ethanol. Diffusion of both solvent components is slowed when they are close to the peptide. Solvent–solute cross relaxation terms for acetic acid in the same solvent obtained from simulations agree with experiment. Preferential interactions of solvent molecules with acetic acid are largely absent, as are effects of this solute on solvent diffusion rates.

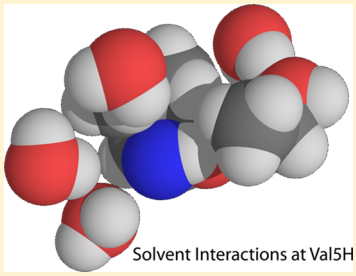

INTRODUCTION

Exposure to ethanol produces a wide variety of effects in living organisms.[1,2] Mixtures of ethanol and water are solvents that can influence stability and conformational properties of biological molecules.[3−6] Use of such solvents in experiments with biomolecules that usually operate in environments that are only partly aqueous may produce results that help in understanding the role(s) of water in maintaining macromolecule structure and activity. In other arenas, mixtures of water and ethanol provide reaction media that enable enzymes to act on substrates that are not soluble in water, although substrate specificity, reaction rates and protein stability may be altered by the solvent mixture. In all of these systems, the effects observed may be the result of direct interactions of solvent alcohol molecules with a protein.

Intermolecular nuclear Overhauser effect (NOE) experiments can be used to examine the interactions of solvents with a dissolved peptide or protein. In previous work, we determined solvent–solute $^1H\{^1H\}$ NOEs for the octapeptide [val5]-angiotensin II (**1**) dissolved in 35% ethanol–water (v/v) at several temperatures.[7,8] A traditional way of interpreting intermolecular solvent–solute NOEs has relied on theoretical descriptions typified by the work of Ayant, et al.[9] In their formulation, the solute proton of interest is considered to be located in a sphere of radius r_{Solute} while the solvent spin is situated in a sphere of radius $r_{Solvent}$. The intermolecular cross relaxation rate is given by

$$\sigma_{HH}^{NOE} = \frac{3\gamma_H{}^4 h^2 N_S}{10\pi D r}(6J_2(2\omega_H) - J_2(0)) \quad (1)$$

where ω_H is the proton Larmor frequency, N_S is the number of solvent spins per mL, D is the sum of the translational diffusion coefficients for the spheres containing the peptide and solvent spins ($D = D_{Solute} + D_{Solvent}$), r is their distance of closest approach ($r = r_{Solute} + r_{Solvent}$) and $J_2(\omega)$ is a spectral density function (eq 2)

$$J_2(\omega) = \left(\left[\omega\tau + \frac{5}{\sqrt{2}}(\omega\tau)^{1/2} + 4\right]/[(\omega\tau)^3 + 4\sqrt{2}(\omega\tau)^{5/2} + 16(\omega\tau)^2 + 27\sqrt{2}(\omega\tau)^{3/2} + 81\omega\tau + 81\sqrt{2}(\omega\tau)^{1/2} + 81]\right) \quad (2)$$

characterized by the correlation time $\tau = r^2/D$.

Equation 1 has been used with experimental bulk translational diffusion coefficients and solvent component concentrations, in concert with reasonable conformations of the peptide, to predict solvent-peptide cross relaxation terms for [val5]angiotensin in 35% ethanol–water.[7,8,10] The results suggested that some interactions of the solvent components with the peptide can be adequately described by the Ayant model. In other instances, this model gave incorrect predictions.

Received: January 22, 2013
Revised: March 6, 2013
Published: March 11, 2013

dx.doi.org/10.1021/jp4007526 | J. Phys. Chem. B 2013, 117, 4880–4892

We now examine the [val5]angiotensin−ethanol−water system through results derived from molecular dynamics simulations at 0 and 25 °C. Both ethanol−peptide and water−peptide intermolecular NOEs were calculated and compared to experimental data as well as the predictions of the Ayant, et al. model. The simulations provide details at the molecular level that help in understanding how the previously reported NOEs arise and, to the extent that the method and parametrization used are valid, provide some insight into the interactions between the peptide and the components of the solvent mixture.

A trace amount of acetate/acetic acid, indicated by a proton nuclear magnetic resonance (NMR) signal near 2.0 ppm was found in the peptide sample used for the experiments. A few simulations of the acetic acid−ethanol−water system were also done to provide a small-molecule comparison to results obtained with the peptide.

H_3N^+−Asp1−Arg2−Val3−Tyr4−Val5−His6−Pro7−Phe8−COO^-

[val5]angiotensin II

1

EXPERIMENTAL SECTION

Experimental cross-relaxation parameters (σ_{HH}^{NOE}) for interactions between solvent CH_3 hydrogens or water hydrogens and hydrogens of [val^5]angiotensin dissolved in 35% ethanol-1,1-d_2−water (v/v) at 273 and 298 K have been previously reported.[7] The water portion of the solvent was a mixture of 85% H_2O and 15% D_2O (v/v). The sample was approximately 10 mM in peptide and contained trace amounts of acetate and 3-(trimethylsilyl)propionic acid-d_4; the apparent pH was 4.0. The reference signal from 3-(trimethylsilyl)propionic acid-d_4 was set to 0.0 ppm.

Molecular Dynamics (MD) Simulations. All simulations were done with the GROMACS package (version 4.5.5)[11,12] running on a SUN SunFire X4600. The AMBER99SB-ILDN force field[13] was used for [val^5]angiotensin and ethanol; ethanol charges were those of Fox and Kollman.[14] The peptide terminals and the Asp, Arg and His side chains were ionized in the model.[15] The TIP4Pew model of water was used.[16]

For simulations of the peptide, a cubic simulation cell, approximately 8.6 nm on a side, was used. It contained a peptide molecule, 2432 ethanol-d_2 molecules, 14440 water molecules and a chloride ion to maintain electrical neutrality. The integration time-step was 0.002 ps. The particle mesh Ewald (PME) method for long-range electrostatics was applied,[17] as was the long-range correction for the van der Waals interaction described by Allen and Tildesley.[18] Cut-offs for electrostatic and van der Waals terms were 1.4 nm. The nonbonded interaction list was updated every 5 steps. Periodic boundary conditions were applied. Motion of the model center of mass was corrected every step. Covalent bonds were constrained to constant length by the LINCS procedure.[19] Systems were regulated at 273 or 298 K and a pressure of 1 bar by use of the Berendsen temperature (velocity rescaling) and pressure coupling methods with relaxation time constants of 0.1 and 1 ps, respectively.[20] Simulations to produce trajectories of 300−600 ns duration were carried out after initial equilibration for at least 2 ns.

Simulations to examine the initial decay of correlation functions took snapshots of trajectories at 0.2 ps intervals. To account for the heterogeneities of the ethanol−water system, 10 different configurations of the system, taken at regular intervals from a 450 ns (273 K) or 300 ns (298 K) duration simulation, were used as starting points for these simulations. Results calculated from the 10 trajectories were averaged. For study of slower phenomena, trajectories of up to 600 ns duration were calculated, with snapshots taken every 5 or 10 ps (298 K) or 15 ps (273 K).

For simulations of acetic acid in 35% ethanol−water, a cubic simulation cell approximately 8.6 nm on a side, was used. The cell contained an acetic acid molecule, 2432 ethanol-d_2 molecules, and 14440 water molecules. The force field parameters for acetic acid were obtained by Dupradeau, et al.[21] and taken from the REDDB Web site (q4md-forcefieldtools.org/REDDb/up/W-46). Simulations used the same procedures as described above, with snapshots of the system taken every 0.25 ps.

Analyses of Trajectories. Programs contained within the GROMACS package were used to compute the system density and self-diffusion coefficients of the solvent components using the Einstein relationship.[22] GROMOS routines were also used for conformational clustering studies and for the calculation of spin coupling constants and conformation-dependent proton chemical shift changes. Locally developed programs were used to determine average interproton distances within the peptide.

Intermolecular dipolar relaxation of a spin A by a collection of identical B spins is given by[10]

$$\sigma_{AB} = \frac{3}{4}\gamma_A^2\gamma_B^2\hbar^2\left\{-\frac{1}{12}J^0(\omega_A - \omega_B) + \frac{3}{4}J^2(\omega_A + \omega_B)\right\} \tag{3}$$

with

$$J^m(\omega) = 2\int_0^\infty G^m(t)e^{-i\omega t}\,dt = 2\int_0^\infty \langle\{\sum_{j\neq i}^{N_{cut}} F_{ij}^m(0)F_{ij}^m(t)\}\rangle e^{-i\omega t}\,dt \tag{4}$$

Gyromagnetic ratios of the spins are γ_A and γ_B and the corresponding Larmor frequencies are ω_A and ω_B. It is assumed that cross-correlation effects can be neglected.[23,24] The correlation functions $G^m(t)$ are written in terms of the components of the vector **r** which connects spin A with a spin B with

$$F^0 = \frac{r^2 - 3z^2}{r^5};\quad F^1 = \frac{z(x - iy)}{r^5};\quad F^2 = \frac{(x - iy)^2}{r^5}$$

Random isotropic motion of the orientation of the vector **r** is assumed; brackets indicate the average of the quantity $F^m(0)F^{m*}(t)$. The strong internuclear distance dependence of $G^m(t)$ encourages limiting the number of B spins considered to those that lie within a cutoff distance (r_{cut}) from the A spin. There will be N_{cut} B spins within this sphere. For the present work, we considered all interactions of a particular solute proton with ethanol CH_3 hydrogens or water hydrogens that were within 3 nm of the target spin. For solutions of the peptide, the number of ethanol methyl hydrogens (N_{cut}) within the 3 nm radius selection sphere at 298 K ranged from 963 to 1523 but averaged 1238 ± 3 (413 ± 1 ethanol molecules). The number of water hydrogens within a 3 nm radius selection sphere at 298 K ranged from 4549 to 5418 and averaged 4986 ± 5 hydrogens. A homogeneous 35% ethanol−water solvent mixture at 298 K containing no peptide has 1264 ethanol methyl hydrogens and 5005 water protons within a 3 nm sphere. The differences between these values and those found are presumably due to the volume occupied by the peptide.

dx.doi.org/10.1021/jp4007526 | J. Phys. Chem. B 2013, 117, 4880−4892

Table 1. Properties of 35 Ethanol–Water (v/v) Solutions

	no solute CH_3CH_2OH/water		acetic acid CH_3CD_2OH/water		[Val5]angiotensin CH_3CD_2OH/water	
property	simulation	experiment	simulation	experiment	simulation	experiment
			At 0 °C			
density (g L^{-1})	967.1 ± 0.4	966.5[a]	980.0 ± 0.1 (967.4[b])	–	980.9 ± 0.1 (968.2[b])	–
$D_{H_2O} \times 10^{10}$ m^2 s^{-1}	5.55 ± 0.10	4.1[c]	5.40 ± 0.10	4.3[d]	5.30 ± 0.07	4.3[d]
$D_{EtOH} \times 10^{10}$ m^2 s^{-1}	3.47 ± 0.11	2.6[c]	3.49 ± 0.10	2.2[d]	3.42 ± 0.13	2.2[d]
$D_{Solute} \times 10^{10}$ m^2 s^{-1}	–	–	2.2 ± 0.1	2.0[d]	0.53 ± 0.07	0.41[d]
			At 25 °C			
density (g L^{-1})	949.0 ± 0.4	952.4[a]	961.4 ± 0.1 (949.0[b])	–	962.3 ± 0.3 (948.9[b])	
$D_{H_2O} \times 10^{10}$ m^2 s^{-1}	13.6 ± 0.16	11,[c] 12[e]	13.4 ± 0.10	11[f]	13.6 ± 0.18	11[g]
$D_{EtOH} \times 10^{10}$ m^2 s^{-1}	8.51 ± 0.26	7.0,[c] 6.4[e]	8.35 ± 0.23	6.8[f]	8.39 ± 0.22	6.8[g]
$D_{Solute} \times 10^{10}$ m^2 s^{-1}	–	–	7.2 ± 0.1	5.0[f]	1.1 ± 0.2	1.4[g]

[a]Value obtained by interpolation of data given in *Lange's Handbook*.[31] [b]Value calculated for the corresponding system containing CH_3CH_2OH. [c]Estimated from the data of Price, et al.[32] [d]Data from Neuman and Gerig.[8] [e]Data from Asenbaum et al.[30] [f]Estimated from the data of Harris et al.[33,34] [g]Data from Gerig.[7]

For isotropic liquids, normalized correlation functions $(G^m(t)/G^m(0))$ are independent of m and have the same time dependence.[25] Following Feller, et al.,[26] we assumed that a normalized function can be represented by a sum of n exponentially decaying functions:

$$\frac{G^m(t)}{G^m(0)} \cong \sum_n a_n \exp\left(-\frac{t}{\tau_n}\right) \tag{5}$$

By approximating the decay of $G^m(t)/G^m(0)$ in this way, the Fourier transform of $G^m(t)$ becomes

$$J^m(\omega) = 2G^m(0)\tau_m(\omega) \tag{6}$$

with

$$\tau_m(\omega) = \sum_n \frac{a_n\tau_n}{(1 + (\omega\tau_n)^2)} \tag{7}$$

where $\sum_n a_n = 1$.

Collecting terms, the intermolecular cross relaxation rate (σ_{HH}^{NOE}) arising from solvent proton-peptide proton interactions is given by

$$\sigma_{HH}^{NOE} = -7.120 \times 10^{-8} G^{\circ}(0)\tau_0(0) + 6.408 \times 10^{-7} G^2(0)\tau_2(2\omega) \tag{8}$$

where time units for the τ_m are ps and the coefficients arise from the constants in eq 3 and various conversion factors.

To compute $G^m(t)$ for a specific proton of the solute, positions of solvent hydrogens within the cutoff distance of the target proton in the simulation box were determined in a trajectory snapshot taken at a time defined as $t = 0$. Diffusion of the selected solvent protons was followed in subsequent snapshots, with the quantities F^0, F^1, and F^2 evaluated at each time step (t). The quantity $F_{ij}^m(0)$ $F_{ij}^m(t)$ was stored for each t. The snapshot chosen to represent $t = 0$ was then advanced one frame along the trajectory and the process repeated. Resulting $F_{ij}^m(0)$ $F_{ij}^m(t)$ values for a given time t were averaged. Typically, for a simulation producing a trajectory of 0.30 μs length and sampled at 10 ps intervals, the correlation function was represented by 1000 points obtained in calculations that averaged about 30 000 evaluations of each time point.

Fitting of $G^m(t)/G^m(0)$ to a sum of exponential functions used a local version of Provencher's program DISCRETE,[27] as described previously.[10] Usually, the optimum fit to the decay of $G^m(t)/G^m(0)$ had three to five exponential terms, with the estimated errors of the fitting parameters ranging from 2% to 6%.

A challenge when computing solvent–solute dipolar interactions from simulations of mixed solvent systems such as the one used in this work is assuring that there is sufficient averaging over the possible configurations of solvent and solute molecules. Simulations were run until there was no significant change in the correlation functions calculated from the MD trajectories, implying that sufficient averaging had taken place.

RESULTS

Computed Solvent Properties. Table 1 compares system density and translational diffusion coefficients computed from simulations of 35% ethanol–water to the corresponding experimental values. Density is predicted well by the simulations but translational diffusion coefficients for solvent molecules are up to about 50% too large.

The enthalpy of mixing for 35% ethanol–water (v/v) at 25 °C, predicted using the method of Dai, et al.[28] from simulations of 2432 ethanol molecules and 14440 water molecules, was −260 J mol^{-1}. This may be compared to the experimental value, −770 J mol^{-1}.[29,30]

While ethanol is miscible with water in all proportions, there is much evidence that these components are incompletely mixed at the microscopic level.[30,35−42] Mass spectral studies indicate that at mole fractions of ethanol near those used for the present work, clusters of up to ∼8 ethanol molecules can be present at 80 °C.[43]

The presence of ethanol clusters in our simulations was examined. Radial distribution functions obtained from X-ray diffraction studies of mixtures of ethanol and water show a collection of features in the range 0.44–0.48 nm which have been assigned to the distances between methyl and methylene carbons of neighboring ethanol molecules.[36,44] Six thousand snapshots from a simulation of the [val5]angiotensin–ethanol–water system at 0 °C were examined, with clustering of ethanol molecules judged by the criterion that at least one carbon–carbon distance between ethanol molecules be less than 0.45 nm. It was found that, on average, about 12% of the ethanol molecules in the simulation were present as single (monomeric) species, while about 8% of the alcohol molecules were present as dimers. Higher order oligomers were also present, with the majority of the ethanol molecules present in clusters of 12 or fewer alcohol molecules. There appears to be little experimental data that is

dx.doi.org/10.1021/jp4007526 | J. Phys. Chem. B 2013, 117, 4880–4892

directly comparable to our system but the heterogeneous nature of the solvent mixture is confirmed.

The distribution of solvent molecules within a 3 nm radius selection sphere around a peptide hydrogen of [val5]angiotensin, while heterogeneous, is highly dynamic. As an example, Figure 1A shows how the solvent composition within a 3 nm sphere

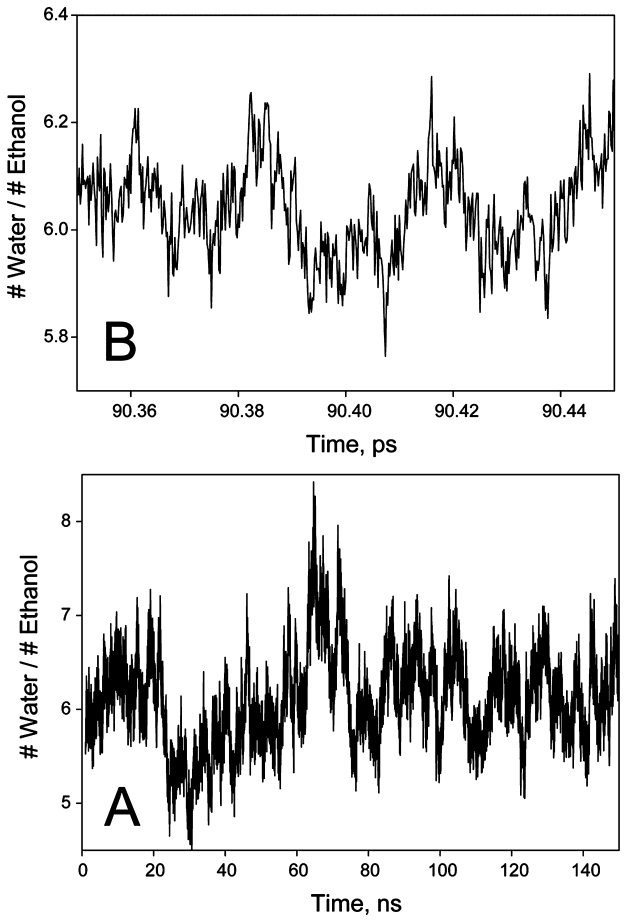

Figure 1. (A) Variation of the ratio of the number of water of molecules to ethanol molecules in a sphere of 3 nm radius centered on the Val5 peptide proton of [val^5]angiotensin in simulations of the system at 25 °C. The configuration of the system was sampled every 5 ps. (B) Variation of the ratio when the system is sampled every 0.2 ps. The ratio of water to ethanol molecules in the bulk solution is 5.938. The data for the plots came from different simulations.

centered on the N−H proton of the Val5 residue of [val^5]angiotensin changes during a 0.3 μs simulation at 25 °C. Figure 1B shows composition variation around the same peptide proton on a narrower time scale. For all protons of the peptide, the number of ethanol molecules relative to water molecules within the 3 nm sphere varies on time scales that range from picoseconds to nanoseconds due to diffusion of the solvent components and the dynamics of cluster formation.

Conformations of [val5]Angiotensin in 35% Ethanol−Water. There are a few signals in the proton NMR spectrum of the peptide arising from a minor conformation (~7%) of the peptide, presumably due to *cis−trans* isomerism at the proline peptide bond.[7] This minor conformation was ignored in the present work. The experimental $^3J_{NHC\alpha H}$ coupling constants for the backbone atoms of the major conformation in 35% ethanol−water range from 7.2 to 9.2 Hz, suggesting that the peptide is predominantly present in extended β-structures.[7] This conclusion is consistent with the paucity of long- and medium-range intramolecular ^{1}H−^{1}H NOEs.[8]

A cluster analyses of the peptide conformations present during MD trajectories at 0 °C was performed using the method described by Daura, et al.[45] Coordinates for the peptides were taken at intervals of 15 ps to provide coordinate sets for as many as 40,000 conformations. These were clustered by comparing the root-mean square deviations (RMSDs) of backbone atoms. Two conformations were considered to be the same when the RMSDs of these atoms in two structures was less than 0.1 nm.

About 25% of all peptide conformations present during 0 °C simulations were represented by a single, extended β-structure, with four other similar β-structures representing about 12%, 9%, 8%, and 7% of the conformations present. Essentially the same number and distribution of conformational clusters were found for simulations of 300, 450, and 600 ns duration at 0 °C, suggesting that the conformations available to the peptide had been adequately sampled by 300 ns.[46]

The five representative conformations of [val^5]angiotensin shown schematically in Figure 2 account for about 60% of

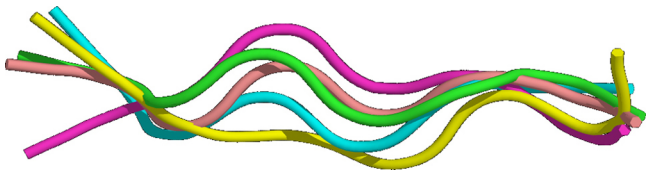

Figure 2. Schematic representation of the dominant conformations of [val^5]angiotensin II at 0 °C in 35% ethanol−water identified by a conformational clustering study done by superimposing backbone structures. Structures 1−5 (colored green, pink, blue, yellow and magenta, respectively) had abundances of approximately 25%, 12%, 9%, 8%, and 7% during a MD trajectory of 0.6 μs duration.

peptide conformations present during 0 °C simulations. These conformations, shown in more detail in the Supporting Information, differ mostly by small variations in conformational angles, with the largest variations present at the amino acid residues near the ends of the peptide.

The effective radii of the structures shown in Figure 2 were calculated by the method previously described.[47] These averaged 0.82 nm, in agreement with the experimental peptide radius estimated from diffusion coefficient determinations (~0.8 nm).[7]

Three-bond $^3J_{NHC\alpha H}$ coupling constants were calculated for simulations at 0 and 25 °C by application of the Karplus-type equation provided by Vuister and Bax.[48] The calculated averaged coupling constants obtained did not appear to depend significantly on the length of a simulation if the simulation duration was greater than 0.15 μs. The average coupling constants obtained were fairly close to the experimental values (Supporting Information) and are consistent with the extended structures shown in Figure 2.

Similarly, Cα−H proton chemical shift changes from random coil values at 25 °C were calculated using the dependence of shifts on the ϕ, ψ conformational angles formulated by Wishart and Nip.[49] These were averaged over the course of a trajectory. Results are given in the Supporting Information. The conformation-dependent shift effects were similar to those calculated for [val5]angiotensin in 25% methanol−water[10] and, although small, were generally in qualitative agreement with experimental results.

Depending on peptide dynamics, intramolecular proton ^{1}H{^{1}H} NOEs for [val5]angiotensin are expected to be

dx.doi.org/10.1021/jp4007526 | J. Phys. Chem. B 2013, 117, 4880−4892

proportional to the average of $1/r_{i,j}^6$ or $1/r_{i,j}^3$ where $r_{i,j}$ is the internuclear distance between two hydrogens.[50] The average of $1/r_{i,j}^6$ and $1/r_{i,j}^3$ was calculated for all proton spin pairs (i, j) of [val^5]angiotensin. Results are given in the Supporting Information. It was found that the average of $1/r_{i,j}^6$ or $1/r_{i,j}^3$ was essentially independent of the duration of a MD trajectory for trajectories longer than 0.1 μs and that $1/r_{i,j}^6$ roughly correlated with observed integrated intensities of NOE cross peaks obtained in NOESY (NOE spectroscopy) studies of the peptide. The calculations indicated that only a few long-range proton−proton NOEs ($>i, i+1$) would be detectable for this system, consistent with experimental observations at 0 and 25 °C.[7]

It can be concluded from consistency of the calculated $^3J_{NHC\alpha H}$, CαH chemical shift changes and ^{1}H−^{1}H intramolecular NOE data with experimental values that the simulations done probably reliably explored the conformations available to [val5]angiotensin in 35% ethanol−water.

Estimated Rotational Correlation Time of the Peptide. The dipole−dipole ^{15}N−^{1}H autocorrelation function for the peptide N−H groups was calculated from the trajectories produced by the simulations of [val5]angiotensin in ethanol−water. This function is expected to be poly exponential, with the most slowly decaying exponential term being related to the correlation time (τ_R) for overall tumbling of the peptide.[51,52] Results are given in the Supporting Information. The average τ_R was 1.4 ns at 0 °C and 0.6 ns at 25 °C. These values are consistent with experimental carbon-13 relaxation studies of [leu5]-angiotensin which gave a τ_R of 0.5 ns at 32 °C.[53] Variation among individual τ_R of [val5]angiotensin presumably reflect differences in local segmental mobility;[54] these local τ_R suggest that the peptide backbone is most rigid near the Val5 residue.

Intermolecular Ethanol−Solute NOEs at 0 °C. Similar to what was observed in the related methanol−water system,[10] the normalized correlation function $G^m(t)/G^m(0)$ for interaction of ethanol CH_3 protons with a peptide hydrogen at 0 °C was found to decay in a few ps to a value near 0.5. Thereafter, the function decayed much more slowly. The correlation function for Val5H-ethanol interactions shown in Figure 3 illustrates these behaviors. Similar results were obtained for ethanol interactions with all peptide protons and with acetic acid.

The rapidly decaying part of the ethanol correlation functions was characterized by an initial decay constant of 5.5−8.5 ps while the time constant τ_0 for the more slowly decaying portion ranged from 70 to 350 ps at 0 °C and 50 to 150 ps at 25 °C. The quantities which characterize the slowly decaying part of correlation functions obtained for interactions of the ethanol (CH_3) hydrogens with hydrogens of the [val^5]angiotensin and acetic acid solutes at 0 °C are collected in Table 2. The corresponding data for the same quantities at 25 °C are given in the Supporting Information.

Figure 4 compares ethanol−peptide hydrogen cross relaxation terms ($\sigma_{CH_3}^{NOE}$) calculated from the MD trajectories and from the theory of Ayant, et al. to experimental results. Interestingly, the cross relaxation parameter for the acetate-acetic acid impurity signal of the sample is predicted well by both approaches. For most peptide backbone hydrogens, predictions of $\sigma_{CH_3}^{NOE}$ using MD simulations and the model of Ayant, et al. are in reasonably good agreement with each other and with experimental results. However, calculated $\sigma_{CH_3}^{NOE}$ for hydrogens on hydrophobic side chains obtained from the MD simulations are too large by up to a factor of 3.

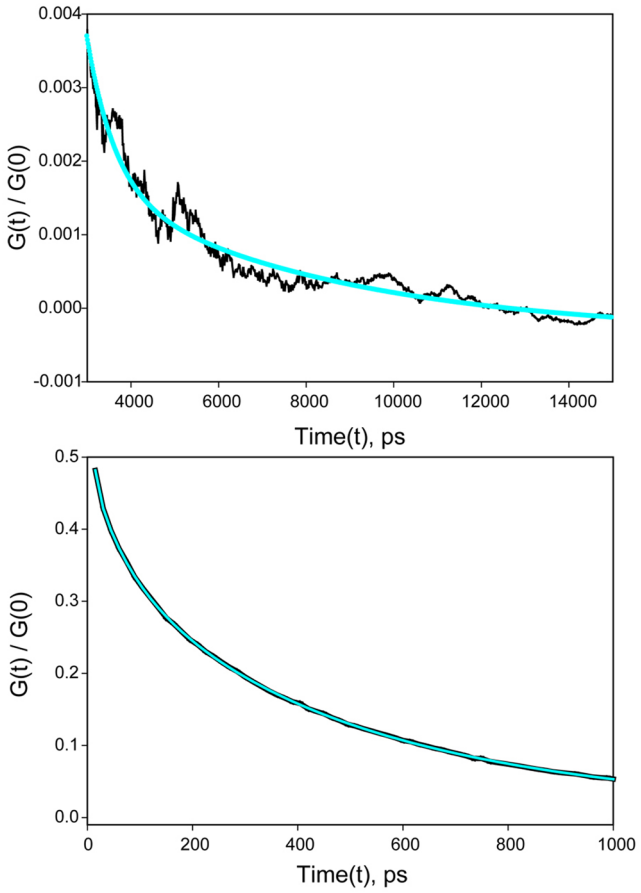

Figure 3. Behavior of the correlation function $G^m(t)/G^m(0)$ for the Val5 NH proton of [val^5]angiotensin as a function of time (black line) at 0 °C. Ignoring data for the first few ps, the function is fit by $[-3.6 \times 10^{-4} + 0.043 \exp(-0.152t) + 0.114 \exp(-0.0167t) + 0.158 \exp(-0.00371t) + 0.223 \exp(-0.00156t) + 0.000338 \exp(-0.000178t)]$ (cyan line). All time units are ps.

Intermolecular Water-Solute NOEs at 0 °C. The water and hydroxyl hydrogens of ethanol give rise to an exchange-averaged solvent signal near 4.9 ppm in solutions of [val5]-angtiotensin in 35% ethanol−water. The cross relaxation rate arising from interactions of these solvent hydroxyl hydrogens will be designated σ_{OH}^{NOE}. Calculation of σ_{OH}^{NOE} for each solute proton from MD simulations involved determining correlation functions for interaction of water hydrogens with peptide hydrogens as well as calculation of functions for interactions of the ethanol hydroxyl hydrogen. Calculated contributions of both to σ_{OH}^{NOE} are given in Table 3, along with σ_{OH}^{NOE} calculated using the approach of Ayant, et al. These quantities are compared to the corresponding experimental data there and in Figure 5.

While some of the experimental and calculated σ_{OH}^{NOE} are in reasonable agreement (Figure 5), others are much more negative than predicted. The averaged NMR signal from solvent water hydrogens and ethanol hydroxyl hydrogens is inverted in experiments to determine σ_{OH}^{NOE}. Exchange of these solvent hydrogens with a peptide hydrogen leads to a negative contribution to the observed cross relaxation term that cannot readily be separated from the portion that is the result of intermolecular solvent−peptide dipole−dipole interactions.[50,55] The negative σ_{OH}^{NOE} observed for ArgH is due to direct exchange with the solvent. Calculations done using a complete relaxation matrix model suggests that negative σ_{OH}^{NOE} values for the

dx.doi.org/10.1021/jp4007526 | J. Phys. Chem. B 2013, 117, 4880−4892

Table 2. Ethanol (CH_3) cross relaxation parameters at 0 °C[a]

hydrogen	$G^0(0) \times 10^{-3}$	$G^2(0) \times 10^{-3}$	$(G_0(0))/(G_2(0))$	fraction[b]	$\tau_0(\omega)$, ps	$\tau_2(\omega)$, ps	$\sigma^{NOE}_{CH_3} \times 10^3$, s^{-1} simulation[c]	eq 1[d]	expt[e]
Asp1HA	1.26	0.859	1.46	0.551	130	25.7	2.6	1.5	~0
Arg2H	1.11	0.689	1.61	0.578	186	28.5	−2.1	0.08	−3.4
Arg2HA	1.53	0.948	1.61	0.560	151	26.4	−0.4	−0.4	−2.6
Val3H	1.13	0.699	1.62	0.617	211	28.9	−4.1	−1.5	−8.3
Val3HA	1.88	1.16	1.63	0.665	175	26.2	−3.9	0.4	−4.3
Val3CH_3	2.97	1.96	1.51	0.500	100	22.9	7.6	1.1	[f]
Tyr4H	1.61	1.05	1.53	0.664	204	27.8	−4.7	−3.0	−6.4[g]
Tyr4HA	1.89	1.25	1.52	0.697	172	25.5	−2.9	−3.0	−4.7
Tyr4Hδ	2.92	1.94	1.50	0.522	114	23.8	5.9	0.03	−1.8
Tyr4Hε	3.17	2.10	1.51	0.515	102	23.3	8.3	1.8	0.4
Val5H	1.26	0.745	1.69	0.656	212	26.5	−6.4	−3.3	−5.8
Val5HA	1.33	0.807	1.64	0.565	215	25.9	−6.9	−0.4	−4.6
Val5CH_3	2.97	1.96	1.51	0.500	100	22.9	7.6	1.1	[f]
His6H	1.02	0.609	1.68	0.593	228	28.3	−5.6	−1.9	−6.4[g]
His6HA	1.14	0.711	1.60	0.603	193	27.7	−3.1	−1.2	−4.4
His6Hδ2	1.20	0.767	1.56	0.571	161	25.8	−1.1	−0.7	1.5
His6Hε1	1.30	0.849	1.53	0.540	132	25.7	1.8	0.2	3.9[h]
Pro7HA	3.27	2.03	1.61	0.471	104	23.0	5.6	−1.1	−2.6
Phe8H	0.503	0.321	1.57	0.702	278	35.8	−2.6	−1.2	−2.1
Phe8HA	1.32	0.844	1.57	0.669	132	27.8	2.6	1.1	−2.6
Phe8Ar	3.24	2.20	1.47	0.424	58.8	20.3	15.1[i]	1.5[i]	5.1[h]
acetic acid	2.75	1.83	1.51	0.462	27.0	13.6	10.6	6.8	8.5

[a]Calculated from a simulation of 0.6 μs duration. [b]Extrapolated intercept for the slow phase of the normalized correlation function. [c]Intermolecular cross relaxation rate calculated using eq 8 and the data given in the table. [d]Intermolecular cross relaxation rate calculated using eq 1 and the model of Ayant et al. with experimental data, as described previously.[7,8] [e]Experimental results from ref 7 and probably reliable to ±25%. [f]Methyl signals were perturbed by the inversion of the solvent methyl signal; the NOE could not be reliably determined. The calculated values are averages of the results for the 12 methyl hydrogens of Val3 and Val5. [g]Signals are overlapped. [h]Signals are overlapped with the Arg2HE and some of the Phe8Ar signals. [i]The calculated values are averages of results for the five aromatic ring protons.

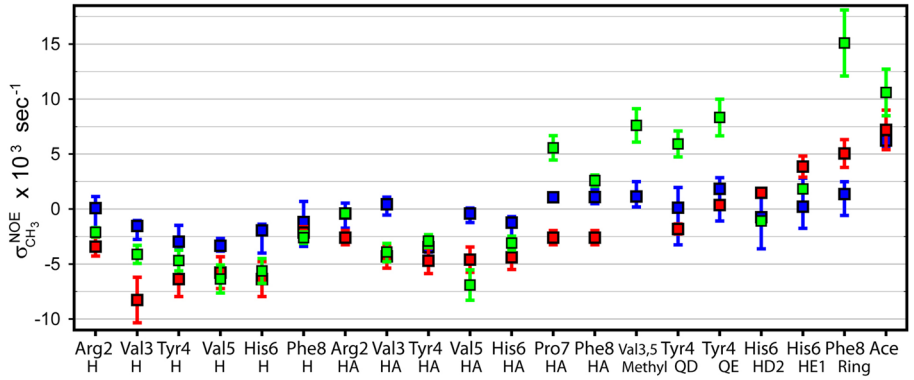

Figure 4. Comparison of experimental ethanol CH_3 hydrogen-solute hydrogen cross relaxation parameters ($\sigma^{NOE}_{CH_3}$) at 0 °C (red squares) to the corresponding parameters calculated using the model of Ayant, et al. (blue squares) and the MD simulations described in the text (green squares). The red bars indicate an experimental uncertainty of ±25%, usually due to signal-to-noise considerations and signal overlap. The results obtained using the Ayant, et al. model are averages of calculations for 10 conformations of the peptide consistent with observed intramolecular NOEs;[7] the blue bars indicate the range from the smallest to the largest $\sigma^{NOE}_{CH_3}$. The green bars indicate the estimated uncertainty in the NOEs obtained from simulations, primarily due to errors in fitting observed correlation functions to obtain τ_0 and τ_2. *Ace* refers to the acetate-acetic acid signal. The *Val3,5 Methyl* and *Phe8Ring* results are the average of results for the valine isopropyl groups and five Phe aromatic hydrogens, respectively. There is no experimental value available for *Val3,5 Methyl* due to distortion of the signals for these hydrogens at ~0.85 ppm by the inversion of the nearby ethanol CH_3 signal and suppression of its carbon-13 sidebands.

hydrogens of the Tyr4 and His6 are consistent with rapid solvent exchange of the acidic protons on the side chains of these amino acids and spin diffusion effects. The σ^{NOE}_{OH} calculated for the Phe8H and PheHA protons using the results of MD simulations show values that are much more negative or positive, respectively, than expected.

Intermolecular Ethanol−Solute and Water−Solute NOEs at 25 °C. Simulations of [val5]angiotensin in 35% ethanol−water (v/v) at 25 °C were used to examine solvent−solute cross relaxation at this temperature. The results are given in the Supporting Information. Overall, it was found that $\sigma^{NOE}_{CH_3}$ parameters for the peptide backbone N−H hydrogens obtained

dx.doi.org/10.1021/jp4007526 | J. Phys. Chem. B 2013, 117, 4880−4892

Table 3. Water Intermolecular Cross-Relaxation Parameters (σ_{OH}^{NOE}) at 0 °C[a]

hydrogen	$G^0(0) \times 10^{-3}$	$G^2(0) \times 10^{-3}$	$(G_0(0))/(G_2(0))$	$\tau_0(\omega)$, ps	$\tau_2(\omega)$, ps	$\sigma_{OH}^{NOE} \times 10^2$, s^{-1} simulation[b]	eq 1[c]	expt[d]
Asp1HA	9.09	6.35	1.43	71.3	37.4	11	3.4	−39
	1.00	0.65	1.54	149	40.9	0.64	0.05	
Arg2H	8.29	5.19	1.60	105	46.5	9.3	2.9	−19
	1.11	6.78	1.64	230	43.7	0.074	0	
Arg2HA	7.44	4.63	1.61	110	48.5	8.6	2.5	2.4
	0.85	0.53	1.62	178	44.3	0.4	−0.01	
Val3H	7.51	4.55	1.65	142	51.1	7.3	1.8	5.9
	1.08	0.68	1.60	238	44.3	0.084	−0.05	
Val3HA	5.74	3.75	1.53	136	50.3	6.6	2.7	1.2
	0.90	0.54	1.68	208	43.1	0.14	0.01	
Val3CH_3	5.80	3.87	1.50	101	41.2	6.0	3.3	3.3[e]
	0.77	0.51	1.51	144	37.8	0.45	0.18	
Tyr4H	7.65	5.12	1.49	135	49.8	9.0	0.71	∼0[f]
	1.30	0.80	1.62	209	41.3	0.19	−0.10	
Tyr4HA	5.29	3.44	1.54	178	50.1	4.3	0.34	−9.8
	0.84	0.58	1.44	231	43.3	0.24	−0.12	
Tyr4Hδ	5.26	3.49	1.50	125	43.6	5.1	2.5	−4.1
	0.81	0.54	1.49	160	67.0	0.14	0.01	
Tyr4Hε	6.62	4.47	1.48	108	42.0	6.9	3.6	−25.
	0.99	0.66	1.49	144	38.1	0.61	0.06	
Val5H	5.99	3.98	1.50	195	49.1	4.2	0.56	2.9
	1.09	0.72	1.53	290	41.9	−0.33	−0.11	
Val5HA	5.56	3.71	1.50	169	50.3	5.2	2.3	∼0
	0.84	0.55	1.52	280	43.	−0.2	−0.01	
Val5CH_3	5.80	3.87	1.50	101	41.2	6.0	3.1	3.3[e]
	0.77	0.51	1.51	144	37.8	0.45	0.03	
His6H	6.65	4.18	1.59	172	47.2	4.5	1.5	∼0[f]
	1.06	0.69	1.54	299	41.1	−0.44	−0.06	
His6HA	3.89	2.55	1.53	191	50.3	2.9	2.0	−15
	0.59	0.40	1.49	242	44.2	0.11	−0.04	
His6Hδ2	6.17	4.09	1.51	140	44.1	5.4	1.6	−59
	0.79	0.50	1.58	236	40.7	−0.026	−0.03	
His6Hε1	12.4	8.19	1.52	79.7	39.2	14	2.7	−27[g]
	0.77	0.50	1.54	139	38.9	0.49	0.07	
Pro7HA	5.65	3.80	1.49	123	43.9	5.8	3.0	5.3
	1.05	0.72	1.47	151	40.3	0.73	0.03	
Phe8H	13.1	7.58	1.73	350	45.3	−11	2.2	11
	1.31	0.57	2.28	393	39.3	−0.22	−0.03	
Phe8HA	11.6	7.62	1.52	106	49.2	15.	3.2	4.0
	0.99	0.63	1.56	136	48.4	1.0	0.04	
Phe8Ar	7.09	4.72	1.50	81.3	32.8	5.8	3.2	[g]
	0.80	0.55	1.47	78.2	33.8	0.74	0.05	
acetic acid	9.11	6.16	1.48	27.4	17.8	5.2	4.3	6.4
	0.86	0.56	1.54	30.9	18.7	0.48	0.2	

[a]Calculated from a trajectory of 0.6 μs duration. The first line for each peptide hydrogen gives the data for interactions of water protons with the indicated hydrogen while the second line gives the corresponding data for interaction of the ethanol hydroxyl groups with the same hydrogen. [b]Intermolecular cross relaxation rate calculated using eq 8 and the data in the Table. [c]Intermolecular cross relaxation rate calculated using eq 2 and the model of Ayant, et al. [d]Experimental results from Gerig;[7] the data include a correction for the deuterium (D_2O) content of the solvent mixture that was not applied in the previous paper. [e]The Val3 and Val5 methyl signals overlapped. The value given is the apparent value for the observed collection of signals. The calculated values are averages of results for the 12 valine methyl hydrogens. [f]The signals for Tyr4H and His5H are overlapped. The value given is the apparent value for the observed signal. [g]The signals for Phe8Ar, Asp2HE, and His5Hε1 are overlapped and values for individual signals could not be reliably determined. The calculated values for Phe8Ar are averages of results for the five aromatic ring protons.

using simulations agree better with the experimental results than do those predicted using the model of Ayant, et al. Values of $\sigma_{CH_3}^{NOE}$ for the backbone HA hydrogens and side chain protons from simulations are larger than the experimental values. Most σ_{OH}^{NOE} obtained from simulations agreed reasonably well with experimental values. Again, the observed σ_{OH}^{NOE} parameters for Arg2H and the Tyr4 and His6 residues showed the effects of exchange with the solvent while the cross relaxation parameters for Phe8H and Phe8HA are predicted by simulations to be about 3 times larger than the experimental values.

Preferential Solvation near the Peptide. To the extent that the MD simulation procedure reliably represents the

dx.doi.org/10.1021/jp4007526 | J. Phys. Chem. B 2013, 117, 4880−4892

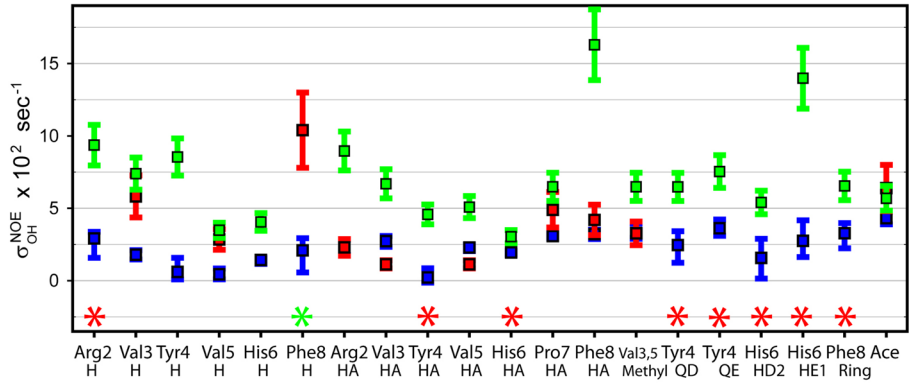

Figure 5. Comparison of experimental water plus ethanol−OH cross relaxation parameters (σ_{OH}^{NOE}) at 0 °C (red squares) to the cross relaxation parameters calculated using the model of Ayant, et al. (blue squares) and obtained using the MD simulations described in the text (green squares). The red bars indicate an experimental uncertainty of ±25%, usually due to signal-to-noise considerations and signal overlap. The results obtained using the Ayant model are averages of calculations for 10 conformations of the peptide consistent with observed intramolecular NOEs; the blue bars indicate the range from the smallest to the largest calculated σ_{OH}^{NOE}. The green bars indicate the estimated uncertainty in the NOEs obtained from simulations, primarily due to errors in fitting observed correlation functions to obtain τ_0 and τ_2. *Ace* refers to the acetate−acetic acid signal. The *Val3,5 Methyl* and *Phe8Ring* results are the average of results for the side chain hydrogens. Experimental values are missing for Tyr4H and His6H because the signals for these hydrogens are nearly coincident and are obscured by the strongly negative signal from the His6HD2 hydrogen. The red asterisks indicate that an experimental σ_{OH}^{NOE} is negative due to hydrogen exchange with solvent hydrogens. The value of σ_{OH}^{NOE} for Phe8H calculated from MD simulations is -11×10^{-2} s^{-1} and is represented by the green asterisk in the plot. An experimental value for σ_{OH}^{NOE} of the Phe8 aromatic protons was not obtainable since the signals for these protons are surrounded and overlapped by strongly negative signals from other protons of the peptide undergoing solvent exchange.

peptide-ethanol−water system examined, the simulations can be used to examine aspects of solvent−solute interactions that are not part of the model of Ayant et al. One assumption of that model is that the solvent is homogeneous throughout the experimental sample.

Preferential interaction of the components of a mixed solvent with a solute is a universal concern in understanding chemical phenomena in such solvents.[56−58] A review by Roccatano includes consideration of experimental and computational approaches used for study of preferential solvation of peptides and proteins.[59] To explore preferential solvent interactions with [val^5]angiotensin, we imagined five concentric spheres (Figure 6) centered on each peptide hydrogen. The diameter of a sphere representing an ethanol molecule is approximately 0.47 nm[7] and the radii of the first four layers shown in the Figures were set to multiples of the ethanol diameter. The last sphere had a radius of 3 nm, corresponding to the cutoff distance used in the peptide-solvent cross relaxation calculations. The ratio of the number of water molecules to number of ethanol molecules in each shell was calculated for each of about 100,000 snapshots taken from simulation trajectories, then averaged. Results at 0 and 25 °C are summarized in Figure 7; more detailed results are given in the Supporting Information.

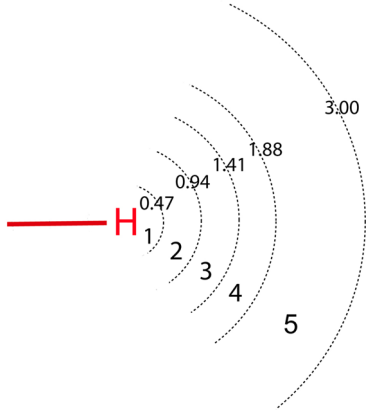

Figure 6. Selection spheres for investigation of solvent interactions with [val^5]angiotensin in 35% ethanol−water. The estimated diameter of a rapidly rotating ethanol molecule is 0.47 nm. A portion of each sphere is occupied by peptide.

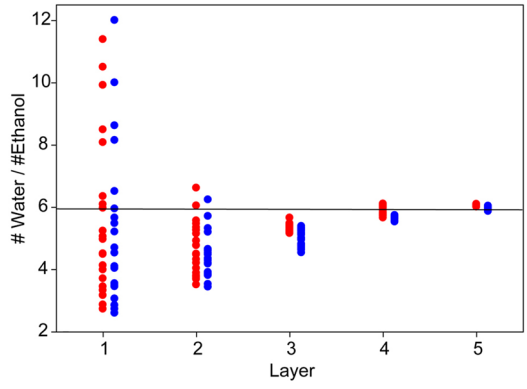

Figure 7. Computed average values of the ratio of the number of water molecules to the number of ethanol molecules ratio in each of the selection layers indicated in Figure 6. Results for 21 backbone and side chain hydrogens of [val5]angiotensin are shown, with red data points representing ratios found at 25 °C and blue points for results at 0 °C. The #water/#ethanol ratio in the simulation box was 5.94 (heavy line). Thus, values of #water/#ethanol less than this correspond to an increased number of ethanol molecules relative to water.

The solvent composition at the outer edge of a 3 nm sphere about a given peptide hydrogen (from 1.88 to 3 nm in Figure 6) had essentially the same ratio of water to ethanol molecules that is present in the full simulation box. This ratio changes as the peptide hydrogen is approached. For most peptide hydrogens, the ratio of water to ethanol molecules falls, indicating that the solvent mixture is richer in ethanol molecules near the surface of the peptide. Preferential interactions with the ethanol of the solvent mixture are particularly noticeable for the side chains of

dx.doi.org/10.1021/jp4007526 | J. Phys. Chem. B 2013, 117, 4880−4892

the valine, tyrosine and phenylalanine residues, presumably a result of the hydrophobicity of these side chains.

The solvent environments around a few peptide hydrogens were found to be richer in water molecules at short distances. These hydrogens include those at or near the N- and C-terminals (Asp1HA, Arg2H, Arg2HA, Phe8HA, Phe8H) and the His6Hε1 side chain hydrogen.

Preferential solvent interactions with acetic acid (the trace impurity present in peptide samples) were also examined. Applying the same methods as indicated above, it was found that the solvent environment near the methyl protons of acetic acid is slightly water-rich.

Orientation of Ethanol at the Peptide Surface. The orientation of ethanol molecules in solvent layer 1 was examined. The number of times solvent ethanol oxygen atoms (N_O) and methyl hydrogens (N_{CH_3}) were within 0.25 nm or less of a peptide hydrogen over the course of a 0.6 μs simulation was evaluated for snapshots of the [val5]angiotensin-ethanol–water system at 0 °C. The ratio N_O/N_{CH_3} should be 1/3 if there is no preferential orientation of the ethanol molecules while values larger than this suggest that the ethanol molecules prefer to be oriented so that their oxygen atoms are within van der Waals contact distance or closer to the peptide hydrogen. Except for the HA hydrogen of Pro7, ethanol molecules near the peptide backbone were preferentially oriented so that the ethanol oxygen atoms are close to the backbone hydrogens. Ethanols near Pro7HA and the hydrogens of hydrophobic side chains preferentially have their methyl groups in contact with these hydrogens. More details regarding these calculations are given in the Supporting Information.

Solvent Diffusion near the Peptide. Solute spin–solvent spin cross relaxation is critically dependent on translational diffusion of solute and solvent species (eq 1). Since diffusion of water molecules near the surface of a protein or peptide appears to be appreciably slowed relative to diffusion in the bulk liquid water,[60] we explored the diffusion of ethanol and water near the surface of [val5]angiotensin.

Translational diffusion coefficients for ethanol and water molecules as a function of their distances from the hydrogens of [val5]angiotensin were computed from simulations using the finite difference expression of Lounnas, et al.[61] It was found that both water and ethanol molecules have diffusion coefficients characteristic of the bulk solvent at distances greater that ~1.6 nm from the peptide but that solvent molecules near the backbone hydrogens of the peptide have translational diffusion coefficients reduced to about 45% of the value for bulk solvent. The reduction is less for solvent molecules near hydrogens of the side chains.

Figure 8 shows typical results of diffusion coefficient calculations for solvent molecules near the Val5H and Tyr4HE protons of the peptide. Although there are small differences in solvent behavior near specific hydrogens of the peptide, ethanol and water molecules approaching backbone protons of the peptide all behave similarly to the distance dependence of the diffusion coefficient shown for Val5H and all side chain protons have diffusion constant-distance dependences similar to those shown for Tyr4HE. More detailed information is given in the Supporting Information.

Ethanol and water solvent translational diffusion coefficients as solvent molecules approach acetic acid were also computed using simulations of the acetic acid–-ethanol–water system. In this case, there was essentially no dependence of the ethanol or water diffusion coefficients on distance from the acetic acid methyl hydrogens (Figure 8).

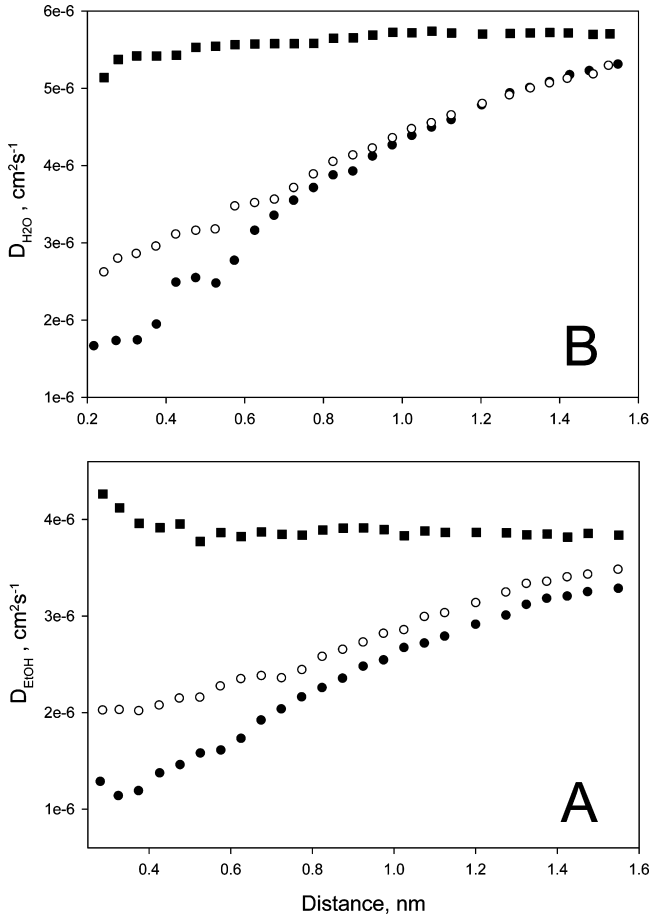

Figure 8. Dependence of the translational diffusion coefficient of ethanol (A) and water (B) as a function of distance from Val5H (filled circles), Tyr4HE (open circles) and acetic acid (filled squares) calculated from simulations in 35% ethanol–water (v/v) at 0 °C.

Long-Lived Interactions. Long-lived ethanol-peptide interactions have been suggested as a possible explanation for disagreements between cross relaxation terms calculated using the Ayant model and experimental observations.[7] The effects of such interactions can be large. For example, a solvent hydrogen interacting with a peptide hydrogen at a distance of 0.3 nm for 6 ns would produce a cross relaxation rate of -78×10^{-3} s^{-1} if the rotational correlation time of the complex is 1.4 ns.

Interactions of specific solvent molecules with [val5]-angiotensin were followed in the simulations to explore possible long-lived solvent encounters. Overall, at 0 °C, it was found that ethanol molecules make 0.3 to 1 contacts per ns with a given peptide proton and that the average duration of a contact is about 0.2 ns. However, some ethanol–peptide contacts persisted for significantly longer times and most hydrogens of the peptide experienced at least one ethanol interaction that lasted for 1 ns or longer.

A typical result of this kind of study is shown Figure 9. The distance between the methyl carbon of a particular ethanol and Val5H was followed as the system evolved. The Figure shows that the methyl group of the chosen ethanol came close to this backbone hydrogen several times during the course of a 0.45 μs simulation, in one instance remaining within contact of Val5H for over 6 ns. However, to be effective in altering the cross-

dx.doi.org/10.1021/jp4007526 | J. Phys. Chem. B 2013, 117, 4880–4892

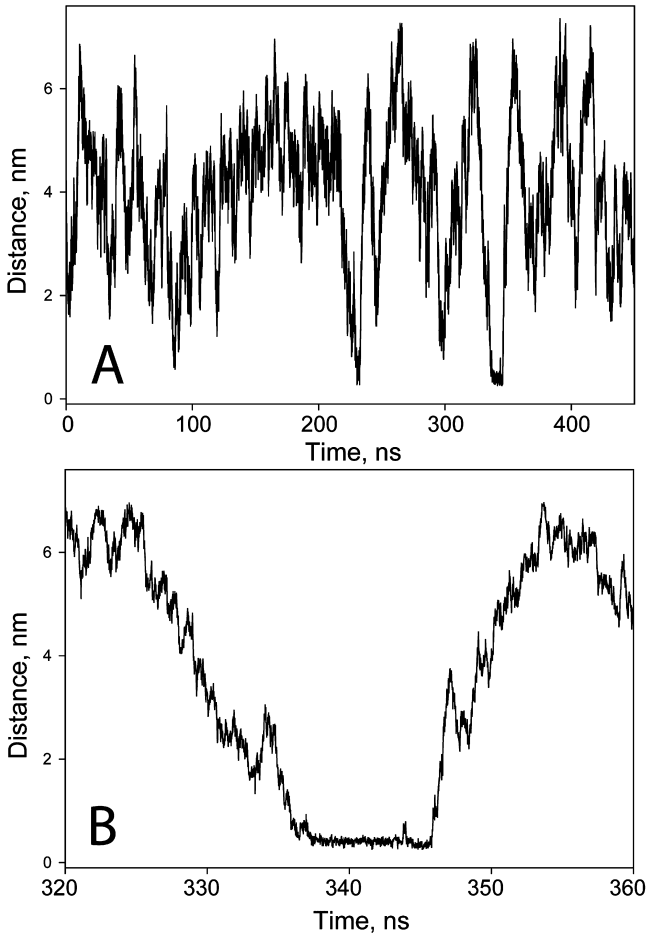

Figure 9. Interaction of a specific ethanol molecule with the Val5H proton at 0 °C. (A) Distance from the peptide proton to the methyl carbon of the ethanol molecule over 450 ns. (B) Expanded view of the distance from the Val5H proton to the methyl carbon of the ethanol molecule. The ethanol molecule remains associated with the peptide for over 6 ns, with the methyl carbon within 0.4 nm or less of the Val5H proton most of this time. However, due to motions within the ethanol–peptide complex, the distance from Val5H to a hydrogen of the ethanol methyl group varied from 0.17 to 0.60 nm.

relaxation rate to the extent suggested above, distances between the solvent hydrogens and a peptide hydrogen have to be nearly constant.[62] Although the ethanol and peptide molecules stayed proximate during the interaction shown, the relative orientations of the molecules did not remain fixed: for the contact shown in Figure 9B, the distances between ethanol methyl hydrogens and Val5H varied randomly between 0.17 and 0.60 nm over the course of the contact.

The influence of various long-lived ethanol-peptide hydrogen interactions on the calculated cross relaxation term ($\sigma_{CH_3}^{NOE}$)was explored in studies that omitted the contribution of a specific ethanol when calculating the dipolar correlation function. Generally, it was found that omitting a single ethanol resulted in changes to $G^0(0)$, $G^2(0)$, $\tau_0(\omega)$ and $\tau_2(\omega)$ of at most a few percent. The contribution of the particular ethanol exhibiting the ~6 ns interaction shown in Figure 9 to the calculated $\sigma_{CH_3}^{NOE}$ for the ethanol–Val5H interaction was about 2%.

Long-lasting interactions of water molecules with the peptide were also observed. These appeared to be about as prevalent as long interactions with ethanol and of about the same average duration. There was no obvious correlation between the average amounts of water and ethanol present near a particular peptide hydrogen and the number or duration of long-lived solvent molecule interactions.

DISCUSSION

As eqs 1 and 2 imply, the mutual diffusion of relaxation partners must be adequately described by a simulation if the NOE is to be reliably predicted. While there have been many attempts to determine properties of ethanol–water mixtures using MD simulations, it has been a challenge to find a set of force field parameters that simultaneously gives a good accounting of translational diffusion coefficients, density, heat of mixing, and other properties.

The enthalpy of mixing we obtained for the 35% ethanol–water is larger than the experimental value. Simulations by Zhang and Yang[38] of 35% ethanol–water using TIP4P water and a united atom model of ethanol also produced an overestimate, about −300 J mol^{-1}, while use of the OPLS force field for ethanol with TIP4P water underestimated the enthalpy of mixing, giving about −1000 J mol^{-1}.[63] The translational diffusion coefficients of ethanol and water found in both studies were ~50 to 80% larger than experimental values. Translational diffusion coefficients obtained from our simulations done using the AMBER parameters for ethanol and the TIP4PEw model of water are in modestly better agreement with experiment.

Our work confirms the microheterogeneity of 35% ethanol–water mixtures and emphasizes the highly dynamic nature of solvent composition throughout the sample and near the surface of [val5]angiotensin. The simulations suggest that, on average, most regions of the octapeptide are preferentially solvated by ethanol molecules. Simulations by others have shown that proteases in 25% ethanol–water (v/v) have a propensity to interact preferentially with ethanol molecules, primarily through van der Waals interactions.[6] Likewise, simulations of a tetrapeptide dissolved in ethanol–water mixtures by Fioroni, et al., indicate preferential accumulation of ethanol near the peptide.[64] These suggestions of preferential interactions of ethanol with peptides and proteins are consonant with experiments indicating preferential binding of ethanol molecules to the surface of lysozyme in ethanol–water mixtures[65,66] and the disaggregation of poly-L-lysines in aqueous solutions of by the addition of ethanol, presumably because the alcohol binds to these materials.[67] The particular blend of hydrophobic and hydrophilic properties present in the ethanol molecule appears to facilitate its interactions with peptide and protein surfaces in competition with interaction with solvent water molecules.

The nature of the dynamics of water molecules near the surface of a biomolecule has been of continuing interest.[68−71] Experiments and MD simulations suggest that water motions are influenced up to ~1 nm away from the surface of these molecules, with water translational diffusion slowed by a factor of 2−3 near the biomolecule surface.[72−74] A part of the reduction of the water translational diffusion coefficient near a protein surface is presumably arises from steric restrictions on motion of solvent molecules due to proximity to the protein[75,76] but electrostatic interactions and hydrogen-bonding appear to guide the bulk of the effect.[73]

Our simulations suggest that translational diffusion of both solvent components in 35% ethanol–water is slowed by about the same extent as the solvent molecules approach the surface of [val5]angiotensin. The influence of the peptide begins to be experienced as far as ~1.5 nm from the peptide surface. Since

dx.doi.org/10.1021/jp4007526 | J. Phys. Chem. B 2013, 117, 4880−4892

ethanol and water molecules interact with each other, it is not clear if the retardation is due to the peptide influencing one solvent component or both. The reduction in diffusion coefficients observed in the simulations brings the local diffusion coefficient closer to the experimental value (Table 1) and is likely a reason that many calculated cross-relaxation rates are in agreement with experimental results and those predicted by the Ayant et al. model.

The small effect of acetic acid on diffusion of nearby solvent molecules (Figure 8) is reminiscent of the effects of a small molecule (maltose) on the diffusion of water calculated by Wang, et al.[77] The more substantial retardation of solvent diffusion near the [val5]angiotensin is presumably due to the larger and more complex long-range electrostatic interactions originating from the peptide.

Although solvent molecule dynamics lead to rapid changes in local solvent composition on the ps time scale (Figure 1), examination of the solvent environment around specific peptide hydrogens of [val5]angiotensin shows that some ethanol or water molecules can remain associated with a peptide hydrogen for several nsec. Because changes in peptide hydrogen-solvent hydrogen distances are limited to some extent during long-lived associations, such interactions lead to increases in the quantities $G^0(0)$ and $G^2(0)$ and tend to lengthen the times $\tau_0(\omega)$ and $\tau_2(\omega)$. Terms based on these factors operate in a contradictory manner in determining a cross relaxation rate (eq 8) and it is thus not possible to state unequivocally how the presence of the long-lived associations of solvent molecules with peptide will affect an observed intermolecular NOE. However, the calculations indicated that in the present system, long-lived association of solvent molecules with the peptide is not a probable reason for disagreements between experimental and predicted cross relaxation terms and, thus, do not support a suggestion made in our previous paper.[7]

While some cross relaxation terms calculated using the MD trajectories agree reasonably well with experimental data (Figures 4 and 5), others do not. Identifying the origins of these failures may point the way to making improvements in the simulations and their analysis to produce better results.

Most striking are the poor predictions of σ_{OH}^{NOE} for the Phe8 backbone hydrogens at both 0 and 25 °C. The factors G^0 (0) and τ_0 (ω) are unusual for these hydrogens compared to others of the backbone (Tables 2 and 3), suggesting aspects of the number, spatial distribution and dynamics of solvent molecules in this part of the peptide are not being correctly captured by the simulations. Inclusion of electrostatic polarization effects offers an avenue for improving the predictions of molecular properties in simulations of ethanol–water mixtures[39,78,79] and peptides.[80,81] It would be interesting to determine the extent to which polarization effects would improve agreement between observed and calculated cross-relaxation rates.

CONCLUSION

Applications of formalisms like that of Ayant, et al. to prediction of dipolar cross relaxation behavior usually make several assumptions about the nature of the solvent–solute system. These include (1) solvent and solute molecules behave as spheres of an appropriate diameter, (2) the composition of the solvent is the same throughout the sample, and (3) the mutual diffusion of solvent and solute molecules can be described by their experimental bulk translational diffusion coefficients. These assumptions have been examined in this work by comparing experimental cross relaxation rates for both components of the 35% ethanol–water solvent mixture and the hydrogens of the peptide [val5]angiotensin to those predicted by the equation of Ayant, et al. and those reckoned from molecular dynamics simulations. The MD results indicate (1) preferential solvation of most of the peptide by ethanol molecules, (2) preferential orientation of ethanol molecules near the peptide backbone, likely facilitating hydrogen bond formation with ethanol, but preferential orientation of ethanol molecules to maximize interaction of the alcohol methyl group with hydrophobic parts of the peptide, and (3) a dependence of the solvent diffusion on the distance between a peptide hydrogen and solvent molecules. Possible effects of these considerations on defining solvent cross relaxation rates with a peptide hydrogen appear to be largely smoothed out by the rapid averaging of solvent molecule positions and orientations. While solvent molecules and the peptide can interact for times as long as several nsec, relaxation effects arising from these interactions are reduced by local reorientation within such complexes. Predicted cross relaxation rates for solvent interactions with the hydrophobic parts of the peptide are less reliable than those for the peptide backbone and may reflect defects in the force field used for the MD simulations.

ASSOCIATED CONTENT

Supporting Information

Illustrations of the structures represented in Figure 1, computed vicinal coupling constants, HA chemical shift increments and intraresidue H–H distances, solvent abundances in the solvent shells indicated in Figure 5, details of parameters derived from simulations used in computing the intermolecular NOEs at 25 °C, data related to the orientation of ethanol near backbone atoms and further details regarding solvent translational diffusion coefficients near the peptide. This material is available free of charge via the Internet at http://pubs.acs.org.

AUTHOR INFORMATION

Corresponding Author

*Telephone: 805-893-2113. Fax: 805-893-4120. E-mail: gerig@chem.ucsb.edu.

Notes

The authors declare no competing financial interest.

ACKNOWLEDGMENTS

We thank the National Science Foundation of support of the initial phases of this work (Grant CHE-0408415) and the authors and developers of GROMACS for making their software available.

REFERENCES

(1) Harris, R. A.; Trudell, J. R.; Mihic, S. J. Ethanol's Molecular Targets. *Sci. Signal* **2008**, *1*, re7.

(2) Eken, A.; Ortiz, V.; Wands, J. R. Ethanol Inhibits Antigen Presentation by Dendritic Cells. *Clin. Vaccine Immunol.* **2011**, *18*, 1157–1166.

(3) Munishkina, L. A.; Phelan, C.; Uversky, V. N.; Fink, A. L. Conformational Behavior and Aggregation of α-Synuclein in Organic Solvents. Modeling the Effects of Membranes. *Biochemistry* **2003**, *42*, 2720–2730.

(4) Pace, C. N.; Trevino, S.; Prabhakaran, E.; Scholtz, J. M. Protein Structure, Stability and Solubility in Water and Other Solvents. *Philos. Trans. R. Soc. London, B* **2004**, *359*, 1225–1235.

(5) Nielsen, J. S.; Buczek, P.; Bulaj, G. Cosolvent-Assisted Oxidative Folding of a Bicyclic α-Conotoxin Iml. *J. Peptide Sci.* **2004**, *10*, 249–256.

(6) Lousa, D.; Baptista, A. M.; Soares, C. M. Analyzing the Molecular Basis of Enzyme Stability in Ethanol/Water Mixtures Using Molecular Dynamics Simulations. *J. Chem. Inf. Model.* **2012**, *52*, 465−473.
(7) Gerig, J. T. Solvent Interactions with [Val^5]Angiotensin II in Ethanol-Water. *J. Phys. Chem. B* **2008**, *112*, 7967−7976.
(8) Neuman, R. C., Jr.; Gerig, J. T. Interaction of Alcohols with [Val^5]Angiotensin in Alcohol-Water Mixtures. *J. Phys. Chem. B* **2010**, *114*, 6722−6731.
(9) Ayant, Y.; Belorizky, E.; Fries, P.; Rosset, J. Effet Des Interactions Dipolaires Magnetiques Intermoleculaires Sur La Relaxation Nucleaire De Molecules Polyatomiques Dans Les Liquides. *J. Phys. (Paris)* **1977**, *38*, 325−337.
(10) Gerig, J. T. Investigation of Methanol-Peptide Nuclear Overhauser Effects through Molecular Dynamics Simulations. *J. Phys. Chem. B* **2012**, *116*, 1965−1973.
(11) van der Spoel, D.; Lindahl, E.; Hess, B.; Groenhof, G.; Mark, A. E.; Berendsen, H. J. C. Gromacs:Fast, Flexible and Free. *J. Computat. Chem.* **2005**, *26*, 1701−1718.
(12) Hess, B.; Kutzner, C.; van der Spoel, D.; Lindhahl, E. Gromacs 4: Algorithms for Highly Efficient, Load Balanced and Scalable Molecular Simulation. *J. Chem. Theory Comput.* **2008**, *4*, 435−447.
(13) Hornak, V.; Abel, R.; Okur, A.; Strockbine, B.; Roitberg, A.; Simmerling, C. Comparison of Multiple AMBER Force Fields and Development of Improved Protein Backbone Parameters. *Proteins: Struct., Funct., Genet.* **2006**, *65*, 712−725.
(14) Fox, T.; Kollman, P. A. Application of the RESP Methodology in the Parametrization of Organic Solvents. *J. Phys. Chem. B* **1998**, *102*, 8070−8079.
(15) Thurlkill, R. L.; Grimsley, G. R.; Scholtz, J. M.; Pace, C. N. pK Values of the Ionizable Groups of Proteins. *Protein Sci.* **2006**, *15*, 1214−1218.
(16) Horn, H. W.; Swope, W. C.; Pitera, J. W.; Madura, J. D.; Dick, T. J.; Hura, G. L.; Head-Gordon, T. Development of an Improved Four-Site Water Model for Biomolecular Simulations: Tip4p-Ew. *J. Chem. Phys.* **2004**, *120*, 9665−9678.
(17) Darden, T.; York, D.; Pederson, L. Particle Mesh Ewald: An N·Log(N) Method for Ewald Sums. *J. Chem. Phys.* **1993**, *98*, 10089−10092.
(18) Allen, M. P.; Tildesley, D. J. *Computer Simulations of Liquids*; Oxford: Oxford, 1987.
(19) Hess, B.; Bekker, H.; Berendsen, H. J. C.; Fraaije, J. G. E. M. Lincs: A Linear Constraint Solver for Molecular Simulations. *J. Computat. Chem.* **1997**, *18*, 1463−1472.
(20) Berendsen, H. J. C.; Postma, J. P. M.; DiNola, A.; Haak, J. R. Molecular Dynamics with Coupling to an External Bath. *J. Chem. Phys.* **1984**, *81*, 3684−3690.
(21) Dupradeau, F.-Y.; Pigache, A.; Zaffran, T.; Savineau, C.; Lelong, R.; Grivel, N.; Lelong, D.; Rosanski, W.; Cieplak, P. The R.E.D. Tools: Advances in RESP and ESP Charge Derivation and Force Field Library Building. *Phys. Chem. Chem. Phys.* **2010**, *12*, 7821−7839.
(22) Leach, A. R. *Molecular Modeling-Principles and Applications*, 2nd ed.; Pearson Prentice Hall: Harlow, England, 2001.
(23) Lippens, G.; Van Belle, D.; Wodak, S. J.; Jeener, J. T_1 Relaxation Time of Water from a Molecular Dynamics Simulation of Water. *Mol. Phys.* **1993**, *80*, 1469−1484.
(24) Odelius, M.; Laaksonen, A.; Levitt, M. H.; Kowalewski, J. Intermolecular Dipole-Dipole Relaxation. A Molecular Dynamics Simulation. *J. Magn. Reson. A* **1993**, *105*, 289−294.
(25) Abragam, A. *The Principles of Nuclear Magnetism*; Oxford: Oxford, U.K., 1961.
(26) Feller, S. E.; Huster, D.; Gawrisch, K. Interpretation of NOESY Cross-Relaxation Rates from Molecular Dynamics Simulation of a Lipid Bilayer. *J. Am. Chem. Soc.* **1999**, *121*, 8963−8964.
(27) Provencher, S. W. An Eigenfunction Expansion Method for the Analysis of Exponential Decay Curves. *J. Chem. Phys.* **1976**, *64*, 2772−2777.
(28) Dai, J.; Li, X.; Zhao, L.; Sun, H. Enthalpies of Mixing Predicted Using Molecular Dynamics Simulations and the OPLS Force Field. *Fluid Phase Equilib.* **2010**, *289*, 156−165.
(29) Boyne, J. A.; Williamson, A. G. Enthalpies of Mixing of Ethanol and Water at 25 C. *J. Chem. Eng. Data* **1967**, *12*, 318.
(30) Asenbaum, A.; Pruner, C.; Wilhelm, E.; Mijakovic, M.; Zoranic, L.; Sokolic, F.; Kezic, B.; Perara, A. Structural Changes in Ethanol-Water Mixtures: Ultrasonics, Brillouin Scattering and Molecular Dynamics Studies. *Vibr. Spectrosc.* **2012**, *60*, 102−106.
(31) Lange, N. A.; Dean, J. A. *Lange's Handbook of Chemistry*, 10th ed.; McGraw-Hill: New York, 1967.
(32) Price, W. S.; Ide, H.; Arata, Y. Solution Dynamics in Aqueous Monohydric Alcohol Systems. *J. Phys. Chem. A* **2003**, *107*.
(33) Harris, K. R.; Newitt, P. J.; Derlacki, Z. J. Alcohol Tracer Diffusion, Density, NMR and FTIR Studies of Aqueous Ethanol and 2,2,2-Trifluoroethanol Solutions at 25 °C. *J. Chem. Soc., Faraday Trans.* **1998**, *94*, 1963−1970.
(34) Harris, K. R.; Newitt, P. J.; Derlacki, Z. J. Alcohol Tracer Diffusion, Density, NMR and FTIR Studies of Aqueous Ethanol and 2,2,2-Trifluoroethanol Solution at 25 °C. *Phys. Chem. Chem. Phys.* **2005**, *7*, 4164.
(35) Nishi, N.; Takahashi, S.; Matsumoto, M.; Tanaka, A.; Muraya, K.; Takamuku, T.; Yamaguchi, T. Hydrogen Bonding Cluster Formation and Hydrophobic Solute Association in Aqueous Solution of Ethanol. *J. Phys. Chem.* **1995**, *99*, 462−468.
(36) Matsumoto, M.; Nishi, N.; Furusawa, T.; Saita, M.; Takamuku, T.; Yamagami, M.; Yamaguchi, T. Structure of Clusters in Ethanol-Water Binary Solutions Studied by Mass Spectrometry and X-Ray Diffraction. *Bull. Chem. Soc. Jpn.* **1995**, *68*, 1775−1783.
(37) Egashira, K.; Nishi, N. Low-Frequency Raman Spectroscopy of Ethanol-Water Binary Solution: Evidence for Self-Association of Solute and Solvent Molecules. *J. Phys. Chem. B* **1998**, *102*, 4054−4057.
(38) Zhang, C.; Yang, X. Molecular Dynamics Simulation of Ethanol/Water Mixtures for Structure and Diffusion Properties. *Fluid Phase Equilib.* **2005**, *231*, 1−10.
(39) Noskov, S.; Lamoureux, G.; Roux, B. Molecular Dynamics Study of Hydration in Ethanol-Water Mixtures Using a Polarizable Force Field. *J. Phys. Chem. B.* **2005**, *109*, 6705−6713.
(40) Wakisaka, A.; Matsuura, K. Microheterogeneity of Ethanol-Water Binary Mixtures Observed at the Cluster Level. *J. Mol. Liq.* **2006**, *129*, 25−32.
(41) Jimenez Rioboo, R. J.; Philipp, M.; Ramos, M. A.; Kruger, J. K. Concentration and Temperature Dependence of the Refractive Index of Ethanol-Water Mixtures: Influence of Intermolecular Interactions. *Eur. Phys. J.* **2009**, *30*, 19−26.
(42) Mijakovic, M.; Kezic, B.; Zoranic, L.; Sokolic, F.; Asenbaum, A.; Pruner, C.; Wilhelm, E.; Perera, A. Ethanol-Water Mixtures: Ultrasonics, Brillouin Scattering and Molecular Dynamics. *J. Mol. Liq.* **2011**, *164*, 66−73.
(43) Nishi, N.; Koga, K.; Ohshima, C.; Yamamoto, K.; Nagashima, U.; Nagami, K. Molecular Association in Ethanol-Water Mixture Studied by Mass Spectrometric Analysis of Clusters Generated through Adiabatic Expansion of Liquid Jets. *J. Am. Chem. Soc.* **1988**, *110*, 5246−5255.
(44) Wertz, D. L.; Kruh, R. K. Reinvestigation of the Structures of Ethanol and Methanol at Room Temperature. *J. Chem. Phys.* **1967**, *47*, 388−390.
(45) Daura, X.; Gademan, K.; Juan, B.; Seebach, D.; van Gunsteren, W. F.; Mark, A. E. Peptide Folding: When Simulation Meets Experiment. *Angew. Chem., Int. Ed.* **1999**, *38*, 236−240.
(46) Smith, L. J.; Daura, X.; van Gunsteren, W. F. Assessing Equilibration and Convergence in Biomolecular Simulations. *Proteins: Struct., Funct., Gene.* **2002**, *48*, 487−496.
(47) Chatterjee, C.; Gerig, J. T. Interactions of Hexafluoroisopropanol with the Trp Cage Peptide. *Biochemistry* **2006**, *45*, 14665−14674.
(48) Vuister, G. W.; Bax, A. Quantitataive J Correlation: A New Approach for Measuring Homonuclear Three-Bond (JH_nH_α) Coupling Constants in ^{15}N-Enriched Proteins. *J. Am. Chem. Soc.* **1993**, *115*, 7772−7777.
(49) Wishart, D. S.; Nip, A. M. Protein Chemical Shift Analysis: A Practical Guide. *Biochem. Cell. Biol.* **1998**, *76*, 153−163.

(50) Neuhaus, D.; Williamson, M. P. *The Nuclear Overhauser Effect in Structural and Conformational Analysis*, 2nd. ed.; Wiley-VCH: New York, 2000.
(51) Lipari, G.; Szabo, A. Model-Free Appoach to the Interpretation of Nuclear Magnetic Resonance Relaxation in Macromolecules. I. Theory and Range of Validation. *J. Am. Chem. Soc.* **1982**, *104*, 4546−4559.
(52) Glore, G. M.; Szabo, A.; Bax, A.; Kay, L. E.; Driscoll, P. C.; Gronenborn, A. M. Deviations from the Simple Two-Parameter Model-Free Approach to the Interpretation of Nitrogen-15 Nuclear Magnetic Resonance Relaxation of Proteins. *J. Am. Chem. Soc.* **1990**, *112*, 4989−4991.
(53) Deslauriers, R.; Paiva, A. C. M.; Schaumburg, K.; Smith, I. C. P. Conformational Flexibility of Angiotensin II. A Carbon-13 Spin-Lattice Relaxation Study. *Biochemistry* **1975**, *14*, 878−886.
(54) Feenstra, K. A.; Peter, C.; Scheek, R. M.; van Gunsteren, W. F.; Mark, A. E. A Comparison of Methods for Calculating Nmr Cross-Relaxation Rates (NOESY and ROESY Intensities) in Small Peptides. *J. Biomol. NMR* **2002**, *23*, 181−194.
(55) Otting, G. NMR Studies of Water Bound to Biological Molecules. *Prog. NMR Spectrosc.* **1997**, *31*, 259−285.
(56) Remerie, K.; Engberts, J. B. F. N. Preferential Solvation of Nonelectrolytes in Mixed Organic Solvents. A Quantitative Approach for B-Disulfones in 1,4-Dioxane-Water, 1,3-Dioxane-Water and Dimethoxyethane-Water in Terms of the Covington Theory. *J. Phys. Chem.* **1983**, *87*, 5449−5455.
(57) Amenta, V.; Cook, J. L.; Hunter, C. A.; Low, C. M. R.; Vinter, J. G. Influence of Solvent Polarity on Preferential Solvation of Molecular Recognition Probes in Solvent Mixtures. *J. Phys. Chem. B* **2012**, *116*, 14433−14440.
(58) Frutos-Puerto, S.; Aguilar, M. A.; Galvan, I. F. Theoretical Study of the Preferential Solvation Effect on the Solvatochromic Shifts of *Para*-Nitroaniline. *J. Phys. Chem. B* **2013**, 2466−2474.
(59) Roccatano, D. Computer Simulations Study of Biomolecules in Non-Aqueous or Cosolvent/Water Mixture Solutions. *Curr. Protein Pept. Sci.* **2008**, *9*, 407−436.
(60) Bagchi, B. Water Dynamics in the Hydration Layer around Proteins and Micelles. *Chem. Rev.* **2005**, *105*, 3197−3219.
(61) Lounnas, V.; Pettitt, B. M.; Phillips, G. N., Jr. A Global Model of the Protein-Solvent Interface. *Biophys. J.* **1994**, *66*, 601−614.
(62) Halle, B. Cross-Relaxation between Macromolecular and Solvent Spins: The Role of Long-Range Dipole Couplings. *J. Chem. Phys.* **2003**, *119*, 12372−12385.
(63) Wensink, E. J. W.; Hoffmann, A. C.; van Maaren, P. J.; van der Spoel, D. Dynamic Properties of Water/Alcohol Mixtures Studied by Computer Simulation. *J. Chem. Phys.* **2003**, *119*, 7308−7317.
(64) Fioroni, M.; Diaz, M. D.; Burger, K.; Berger, S. Solvation Phenomena of a Tetrapeptide in Water/Trifluoroethanol and Water/Ethanol Mixtures: A Diffusion NMR, Intermolecular NOE and Molecular Dynamics Study. *J. Am. Chem. Soc.* **2002**, *124*, 7737−7744.
(65) Lehmann, M. S.; Mason, S. A.; McIntyre, G. J. Study of Ethanol-Lysozyme Interactions Using Neutron Diffraction. *Biochemistry* **1985**, *24*, 5862−5869.
(66) Ortore, M. G.; Mariani, P.; Carsughi, F.; Cinelli, S.; Onori, G.; Teixeira, J.; Spinozzi, F. Preferential Solvation of Lysozyme in Water/Ethanol Mixtures. *J. Chem. Phys.* **2011**, *136*, 245103.
(67) Sabate, R.; Estelrich, J. Diaggregating Effects of Ethanol at Low Concentration on B-Poly-L-Lysines. *Int. J. Biol. Macromol.* **2003**, *32*, 10−16.
(68) Makarov, V. A.; Feig, M.; Andrews, B. K.; Pettitt, B. M. Diffusion Study of Solvent around Biomolecular Solutes. A Molecular Dynamics Simulation Study. *Biophys. J. 75*, 75, 150−158.
(69) Nandi, N.; Bhattacharyya, K.; Bagchi, B. Dielectric Relaxation and Solvation Dynamics of Water in Complex Chemical and Biological Systems. *Chem. Rev.* **2000**, *100*, 2013−2045.
(70) Bizzarri, A. R.; Cannistraro, S. Molecular Dynamics of Water at the Protein-Solvent Interface. *J. Phys. Chem. B* **2002**, *106*, 6617−6633.
(71) Qvist, J.; Persson, E.; Mattea, C.; Halle, B. Time Scales of Water Dynamics at Biological Interfaces: Peptides, Proteins and Cells. *Faraday Discuss.* **2009**, *141*, 131−144.
(72) Modig, K.; Liepinsh, E.; Otting, G.; Halle, B. Dynamics of Protein and Peptide Hydration. *J. Am. Chem. Soc.* **2004**, *126*, 102−114.
(73) Pizzitutti, F.; Marchi, M.; Sterpone, F.; Rossky, P. J. How Protein Surfaces Induce Anamalous Dynamics of Hydration Water. *J. Phys. Chem. B* **2007**, *111*, 7584−7590.
(74) Mattea, C.; Quist, J.; Halle, B. Dynamics of Protein-Water Interface from ^{17}O Spin Relaxation in Deeply Supercooled Solutions. *Biophys. J.* **2008**, *95*, 2951−2953.
(75) Callaghan, P. T. *Pinciples of Nuclear Magnetic Resonance Microscopy*; Clarendon: Oxford, 1993.
(76) Van Geldren, F.; DesPres, D.; van Zijl, P. C. M.; Moonen, C. T. W. Evaluation of Restricted Diffusion in Cylinders. Phosphocreatine in Rabbit Leg Muscle. *J. Magn. Res. B* **1994**, *103*, 255−260.
(77) Wang, C. X.; Chen, W. Z.; Tran, V.; Douillard, R. Analysis of Interfacial Water Structure and Dynamics in α-Maltose Solution by Molecular Dynamics Simulatoin. *Chem. Phys. Lett.* **1996**, *251*, 268−274.
(78) Ren, P.; Wu, C.; Ponder, J. W. Polarizable Atomic Multipole-Based Molecular Mechanics for Organic Molecules. *J. Chem. Theory Computat.* **2011**, *7*, 3143−3161.
(79) Zhong, Y.; Patel, S. Electrostatic Polarization Effects and Hydrophobic Hydrationin Ethanol-Water Solutions from Molecular Dynamics Simulations. *J. Phys. Chem. B* **2009**, *113*, 767−778.
(80) Lopes, P. E. M.; Roux, B.; MacKerell, J. A. D. Molecular Modeling and Dynamics Studies with Explicit Inclusion of Electronic Polarizability. Theory and Applications. *Theor. Chem. Acc.* **2009**, *124*, 11−28.
(81) Kucukkal, T. G.; Stuart, S. J. Polarizable Molecular Dynamics Simulations of Aqueous Peptides. *J. Phys. Chem. B* **2012**, *116*, 8733−8740.